

ELECTRONIC SUPPLEMENTARY INFORMATION FOR:

In the search of widening the electrochemical window of solid electrolytes for Li-batteries: the $\text{La}_{0.29}\text{Li}_{0.12+x}\text{M}_{1-x}\text{Zr}_x\text{O}_3$ ($\text{M} = \text{Nb}, \text{Ta}$) perovskite-type systems.

Ester García-González,^a Rafael Marín-Gamero,^a Miguel Kuhn-Gómez,^a Alois Kuhn,^b Flaviano García-Alvarado,^b Susana García-Martín*,^a

^a Departamento de Química Inorgánica I, Facultad de Ciencias Químicas, Universidad Complutense, 28040 Madrid, Spain

^b Departamento de Química y Bioquímica, Facultad de Farmacia, Universidad San Pablo-CEU, CEU Universities, Urbanización Montepríncipe, Boadilla del Monte, E-28668, Madrid, Spain

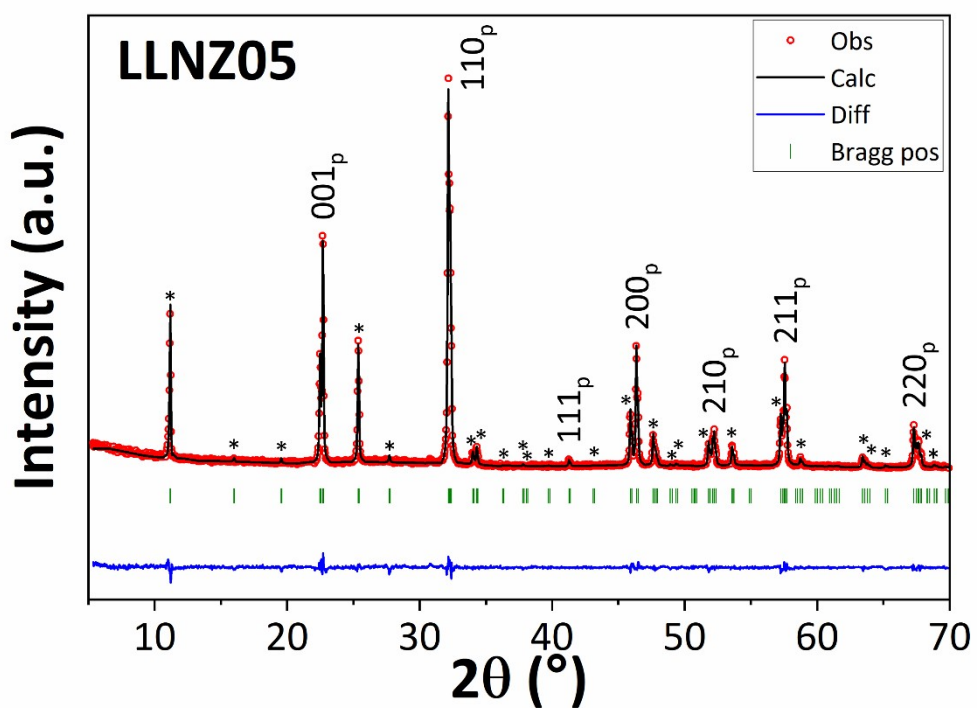
Figures

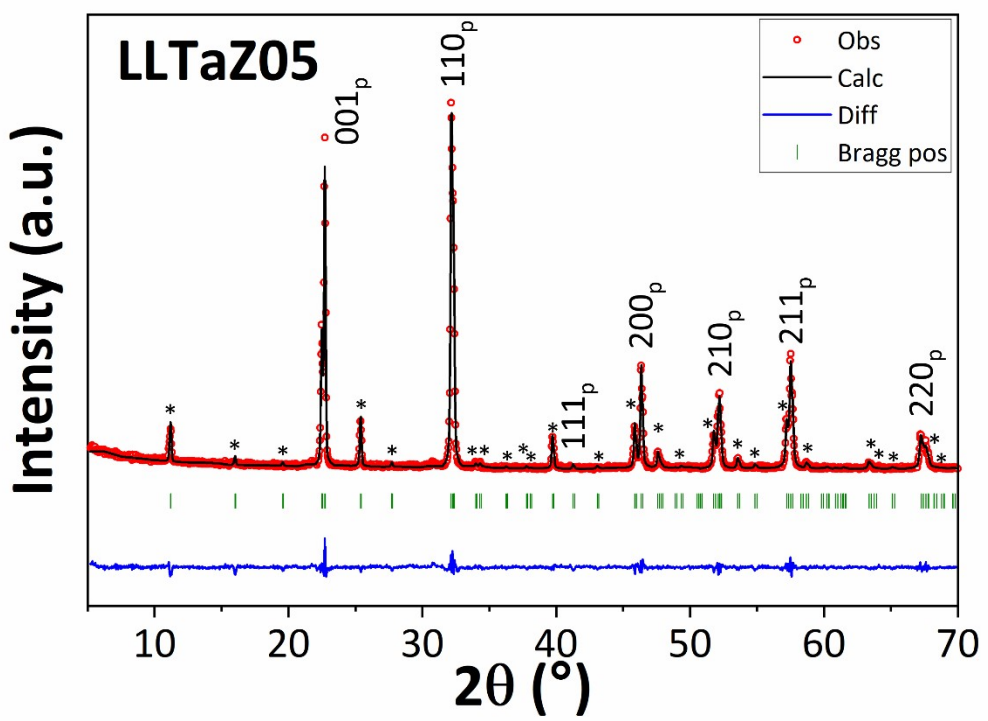
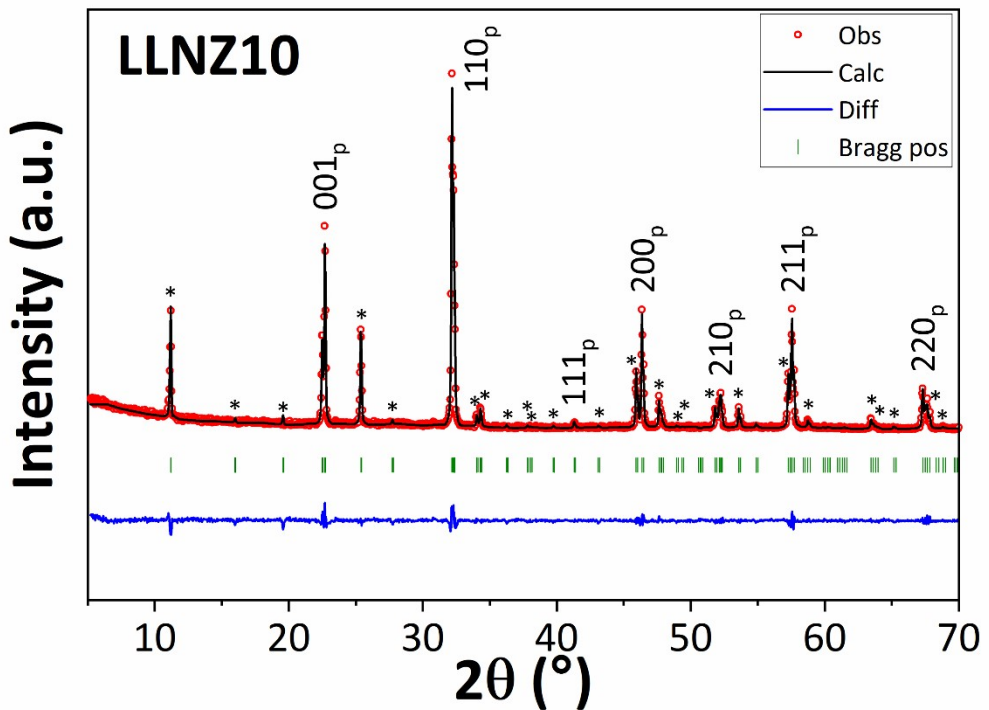
Figure S1	Le Bail analysis of the PXRD patterns of the synthesized oxides.
Figure S2	(a) Complex impedance diagrams of LLNO at 298 K and 373 K. (b) Z'' and M'' vs frequency at 298 K of LLNO.
Figure S3	Cyclic voltammograms of LLTaZ05 and blank.

Tables

Table S1	Atomic percentages of the synthesized oxides determined by XEDS.
Table S2	Unit cell parameters as provided by Le Bail analysis of the PXRD patterns.
Table S3	Resistance and capacitance values at different temperatures of the oxides as obtained from the Nyquist and the Bode diagrams.

Figure S1. Le Bail analysis of the PXRD patterns of the synthesized oxides. The red circles denote the observed data, the black lines represent the refined profile. The positions of Bragg reflections are plotted in green; the blue lines correspond to the difference between the calculated and observed PXRD patterns. The patterns have been fitted according to the SAED and HRTEM results that show a weak modulation of the crystal structure associated to the combination of the tilting of the oxygen-octahedra network modulation with the compositional modulation, leading to the $\sqrt{2}a_p \times \sqrt{2}a_p \times 2a_p$ unit cell. The Miller indices correspond to the cubic perovskite cell and superstructure diffraction maxima are marked with asterisks. Profile fitting has been done according to the P1 space group, since the complex micro/nanostructure of the samples (see main text), hinders the accurate determination of the space group.





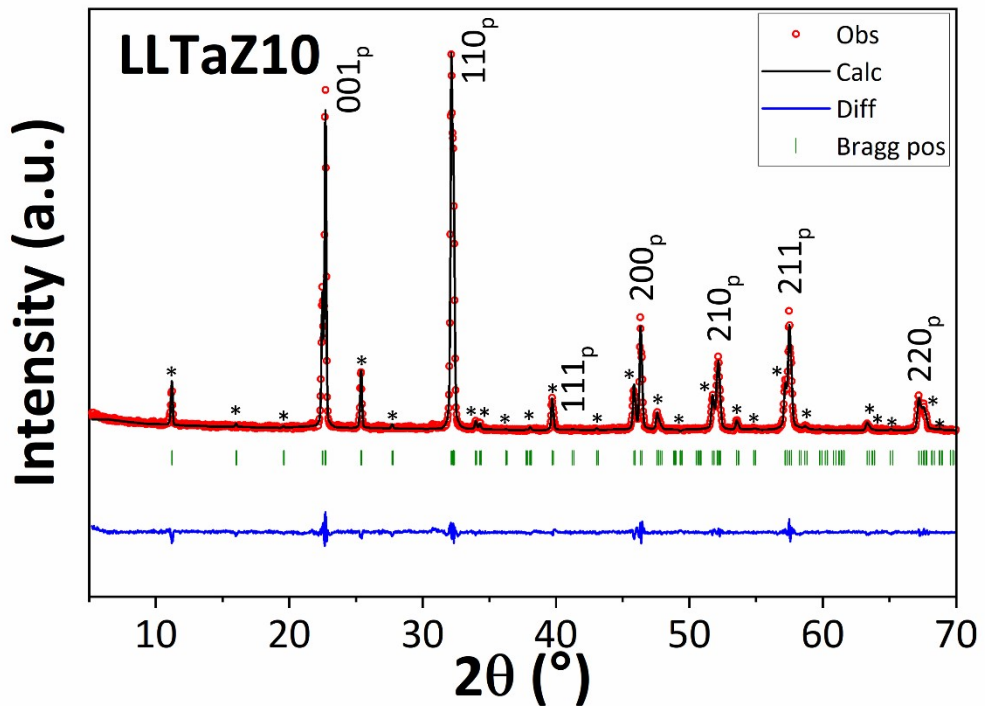


Figure S2. (a) Complex impedance diagrams of LLNO at 298 K and 373 K. (b) Z'' and M'' vs frequency at 298 K of LLNO

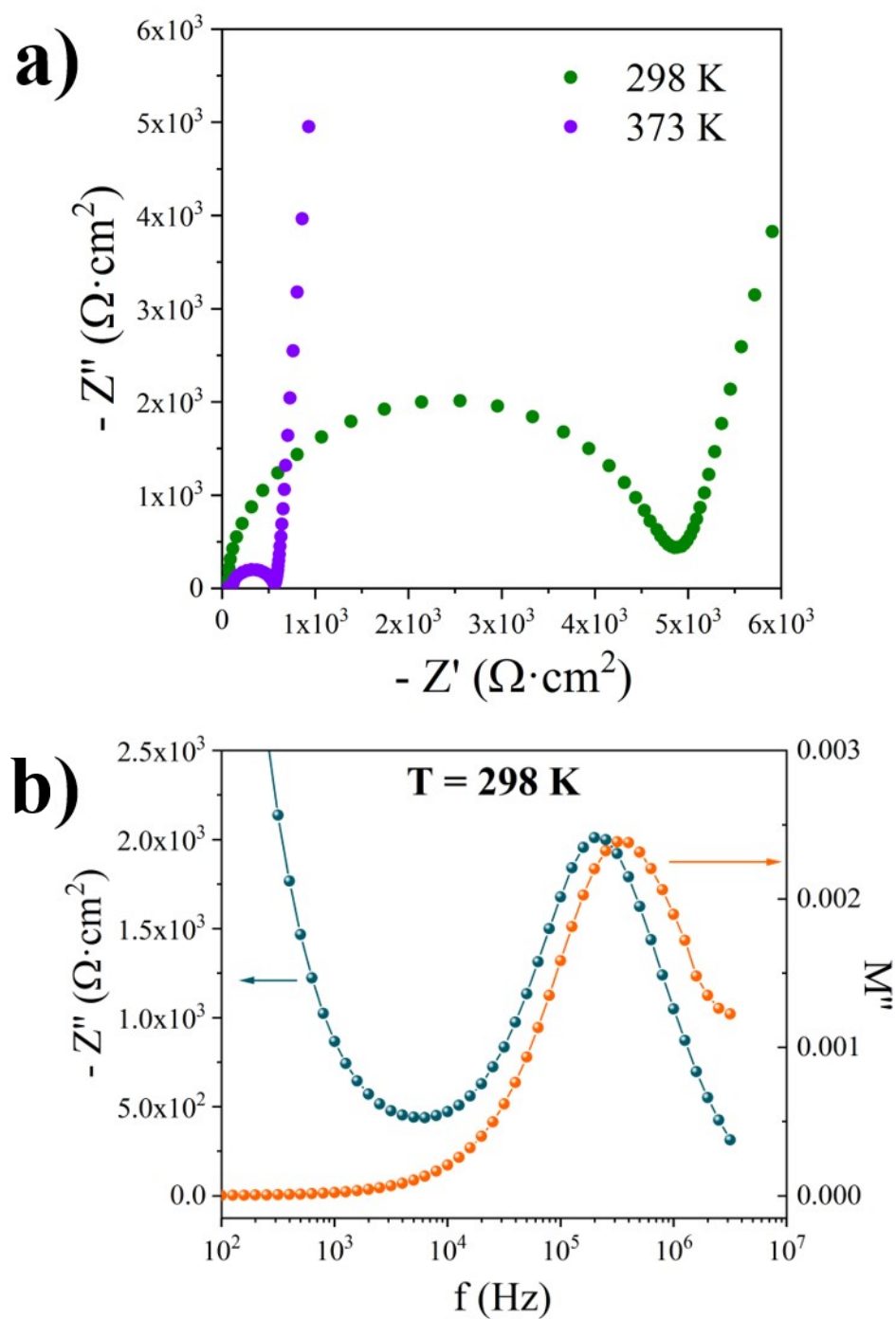


Figure S3. Cyclic voltammograms of LLTaZ05 and blank in the 0-3 V voltage range (a and c) and in the 3.0-5.0 V voltage range (b and d).

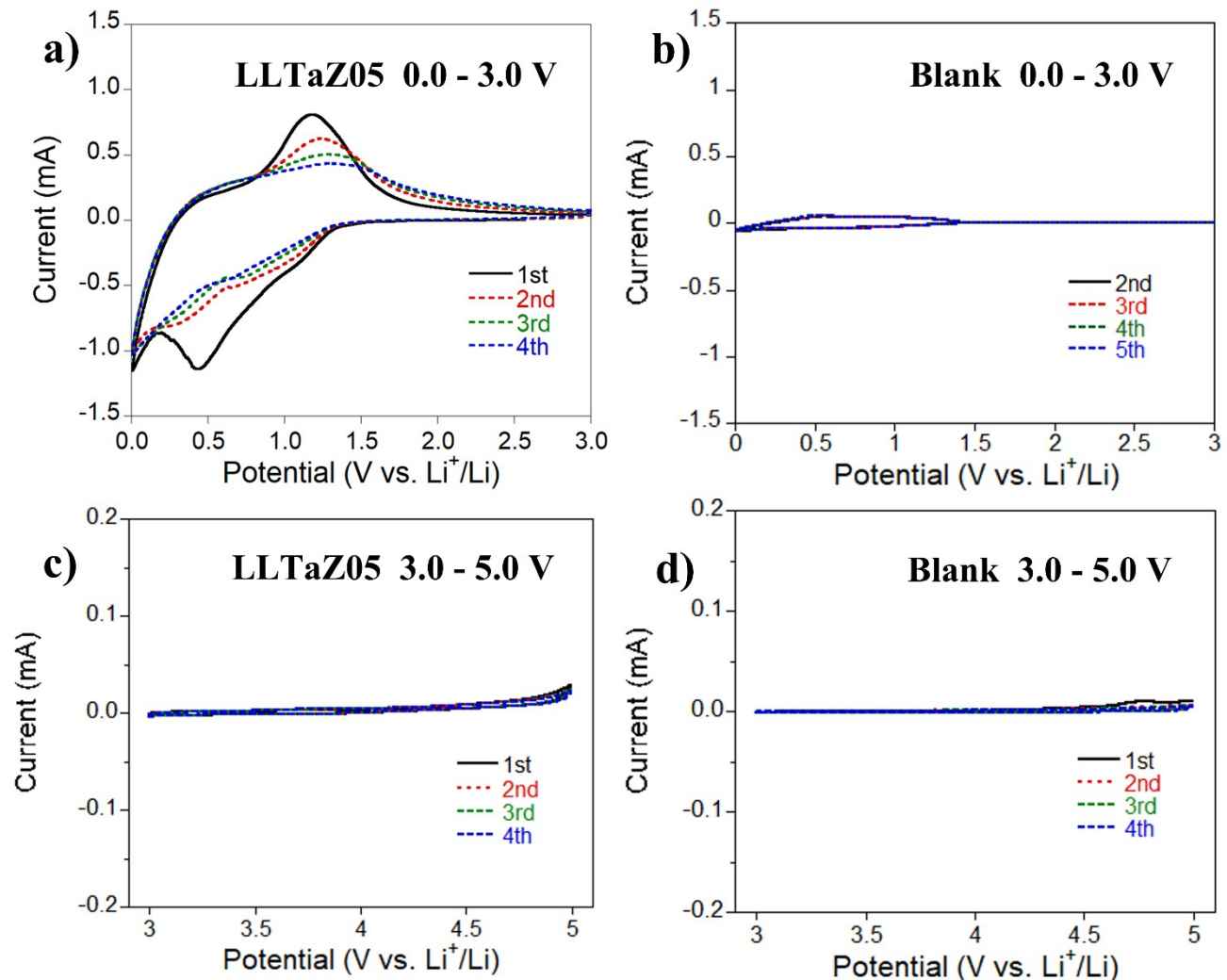


Table S1. Atomic percentages of lanthanum, niobium (tantalum) and zirconium of the synthesized oxides, as determined by XEDS in TEM-mode (average values from about 50 analysed crystals).

	LLNZ05		LLNZ10	
	Nominal	Analytical	Nominal	Analytical
La	22.66	21.02	22.66	23.22
Nb	73.47	74.70	69.60	70.51
Zr	3.86	4.28	7.73	6.27

	LLTaZ05		LLTaZ10	
	Nominal	Analytical	Nominal	Analytical
La	22.66	24.20	22.66	23.01
Ta	73.47	72.98	69.60	70.50
Zr	3.86	2.83	7.73	6.49

Table S2. Unit cell parameters of the synthesized oxides as provided by Le Bail analysis of the PXRD patterns.

<i>P1</i>	LLNO¹	LLNZ05	LLNZ10	LLTaZ05	LLTaZ10
a (Å)	5.525(6)	5.534(0)	5.534(3)	5.540(1)	5.543(5)
b (Å)	5.59(1)	5.532(8)	5.535(1)	5.539(2)	5.540(5)
c (Å)	7.837(7)	7.899(2)	7.896(8)	7.912(1)	7.918(1)
χ^2		3.94	2.50	2.32	2.30

1 S. García-Martín, J. M. Rojo, H. Tsukamoto, E. Morán and M. A. Alario-Franco, *Solid State Ionics*, 1999, **116**, 11–18.

Table S3. Total resistance, conductivity and capacitance values at different temperatures of the studied oxides, obtained from the Nyquist and the Bode diagrams. Notice that two resistance values are determined for LLTaZ10 at 300 K, the resistance associated to “bulk” at $\sim 10^5$ Hz and the resistance associated to grain boundaries at ~ 1 Hz. The resistance of the grain boundaries is one order of magnitude higher than the one of the “bulk”.

LLNO

T (K)	R _{Bode} (Ω)	σ _{Bode} (S.cm ⁻¹)	R _{Nyquist} (Ω)	σ _{Nyquist} (S.cm ⁻¹)	C (F)
298	4043	3.17E-5	4853.6	2.64E-5	1.86E-9
305	3490	3.68E-5	4201.3	3.06E-5	1.84E-9
315	2243	5.72E-5	2712.7	4.73E-5	1.83E-9
335	1257	1.02E-4	1549.7	8.28E-5	1.81E-9
354	754.5	1.70E-4	957.54	1.34E-4	1.85E-9
373	--	--	562.02	2.28E-4	1.86E-9

LLNZ05

T (K)	R _{Bode} (Ω)	σ _{Bode} (S.cm ⁻¹)	R _{Nyquist} (Ω)	σ _{Nyquist} (S.cm ⁻¹)	C (F)
298	5454	4.49E-05	7104.4	3.45E-05	2.07E-09
305	4916	4.98E-05	5839.2	4.20E-05	2.07E-09
315	1312	1.87E-04	3987.1	6.14E-05	2.06E-09
333	1559.6	1.57E-04	2108.8	1.16E-04	2.06E-09
353	660.8	3.71E-04	994.52	2.46E-04	2.16E-09
373	245.2	9.99E-04	495.67	4.94E-04	--

LLNZ10

T (K)	R _{Bode} (Ω)	σ _{Bode} (S.cm ⁻¹)	R _{Nyquist} (Ω)	σ _{Nyquist} (S.cm ⁻¹)	C (F)
300	8445	2.42E-05	10157	2.01E-05	1.97E-09
325	3073	6.65E-05	3767.6	5.42E-05	1.94E-09
348	1288	1.59E-04	1650.7	1.24E-04	1.92E-09
373	483	4.22E-04	766.62	2.67E-04	1.96E-09
400	126	1.62E-03	365.49	5.59E-04	--
423	--	--	189.67	1.08E-03	--

LLTaZ05

T (K)	R _{Bode} (Ω)	σ _{Bode} (S.cm ⁻¹)	R _{Nyquist} (Ω)	σ _{Nyquist} (S.cm ⁻¹)	C (F)
300	34484	5.93E-06	39857	2.67E-06	2.79E-10
325	9785	2.09E-05	11554	9.21E-06	2.62E-10
348	4671	4.37E-05	5663.2	1.88E-05	2.67E-10
373	1924	1.06E-04	2696.6	3.94E-05	2.83E-10
398	772.0	2.65E-04	1537.7	6.92E-05	--
423	346.3	5.90E-04	826.62	1.29E-04	--

LLTaZ10

T (K)	R _{Bode} (Ω)	σ _{Bode} (S.cm ⁻¹)	R _{Nyquist} (Ω)	σ _{Nyquist} (S.cm ⁻¹)	C (F)
300	21580 (~10 ⁵ Hz) 426136 (~1 Hz)	7.74E-6(~10 ⁵ Hz) --	26795 --	6.23E-06 --	2.79E-10 --
325	10370	1.61E-5	13102	1.27E-05	--
350	5652	2.95E-5	7309	2.28E-05	--
375	2888	5.78E-5	4114	4.06E-05	--
397	1418	1.18E-4	2322.2	7.19E-05	--
423	540	3.09E-4	1018.5	1.64E-04	--

Oxide	E _a (eV)
LLNO	0.28
LLNZ05	0.34
LLNZ10	0.24
LLTaZ05	0.34
LLTaZ10	0.30